

Multi-vortex states of a thin superconducting disk in a step-like external magnetic field

M. V. Milošević*, S. V. Yampolskii# and F. M. Peeters
*Departement Natuurkunde, Universiteit Antwerpen (UIA),
 Universiteitsplein 1, B-2610 Antwerpen, Belgium*
 (November 2, 2018)

The vortex states in a thin mesoscopic disk are investigated within the phenomenological Ginzburg-Landau theory in the presence of a step-like external magnetic field with zero average which could model the field resulting from a ferromagnetic disk or a current carrying loop. The regions of existence of the multi-vortex state and the giant vortex state are found. We analyzed the phase transitions between them and found regions in which ring-shaped vortices contribute. Furthermore, we found a vortex state consisting of a central giant vortex surrounded by a collection of anti-vortices that are located in a ring around this giant vortex.

I. INTRODUCTION

Recent progress in microfabrication and measurement techniques makes it possible to study the properties of mesoscopic superconducting samples, and, in particular, disks with sizes comparable to the penetration depth λ and the coherence length ξ [1–6]. Depending on the disk size various superconducting states can exist in such samples in an external magnetic field.

In small disks, where the confinement dominates, there exist only giant vortex (*GV*) states (circular symmetric states with a fixed value of angular momentum L) [2,7]. For sufficiently large disks the *GV* state can break up into the multi-vortex (*MV*) state (a mixture of giant vortices with different angular momentum) [3,4]. Also ring-shaped vortex states with larger energy than *GV* and *MV* ones were predicted [8]. These ring-shaped two-dimensional vortex states have a cylindrically symmetric magnetic field profile and they are different from the ring-vortices that were e.g. found in three-dimensional superfluid liquid helium. But the analysis of Ref. [6] showed that in a superconducting disk in the presence of a homogeneous magnetic field the ring-shaped vortices are unstable.

In the present paper we study the *MV* states of a thin superconducting disk in an inhomogeneous magnetic field \vec{H}_0 with step-like profile. This magnetic field profile could approximate the field resulting from a magnetic dot (they are usually used in experiments, e.g. see Ref. [9]) as well as the field of a current loop (Fig. 1). We found that this model field profile captures a lot of interesting physics and that the step height and width strongly influence the superconducting phase diagram.

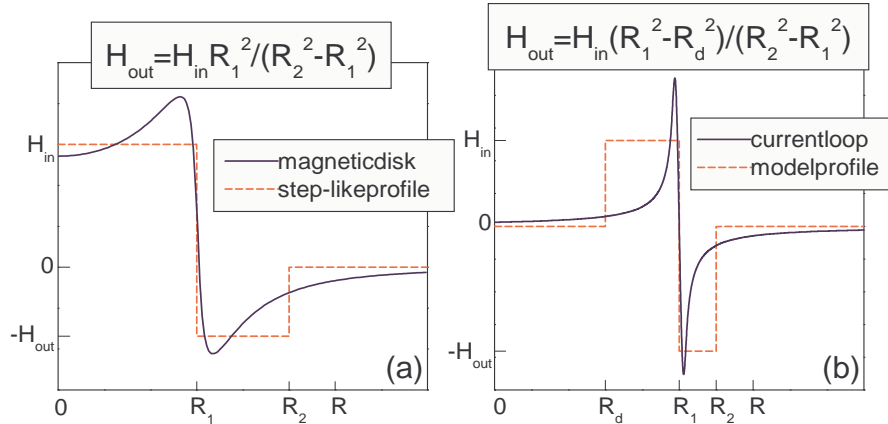


FIG. 1. The magnetic field profile from a magnetic disk (a) and a current loop (b) and the corresponding step field models.

II. APPROACH USED

The details of our approach can be found in Refs. [3,4,6] and, therefore, we briefly sketch only the necessary steps. We restrict ourselves to sufficiently thin disks such that $d \ll \xi, \lambda$. In this case, to a first approximation, the magnetic field due to the circulating superconducting currents may be neglected and the magnetic field inside the disk equals

the external one. Following Refs. [3–6], the order parameter of the MV state is written as a linear combination of eigenfunctions of the *linearized* Ginzburg-Landau equation

$$\psi(\vec{\rho}) = \sum_{L_j=0}^L \sum_{n=0}^{\infty} C_{n,L_j} f_{n,L_j}(\rho) \exp(iL_j\varphi), \quad (1)$$

where ρ is the radial distance from the disk center, φ is the azimuthal angle, and n enumerates the different radial states for the same L_j . In the homogeneous magnetic field case L is the value of the effective total angular momentum which is equal to the number of vortices in the disk. Later we will see that, for our inhomogeneous magnetic field case, the assignment of the total vorticity can be tricky.

Substituting Eq. (1) in the free energy (measured in $F_0 = H_c^2 V / 8\pi$ units)

$$F = \frac{2}{V} \left\{ \int dV \left[-|\psi|^2 + \frac{1}{2} |\psi|^4 + \left| -i\vec{\nabla}\psi - \vec{A}\psi \right|^2 + \kappa^2 \left(\vec{h}(\vec{\rho}) - \vec{H}_0 \right)^2 \right] \right\}, \quad (2)$$

(here $\vec{h}(\vec{\rho}) = \vec{\nabla} \times \vec{A}(\vec{\rho})$ is the local magnetic field, \vec{A} is the vector potential) we obtain F as a function of the complex parameters C_{n,L_j} . Minimization of F with respect to these parameters allows to find the equilibrium vortex configurations and to determine their stability.

We restrict ourselves to states built up by only two components in Eq. (1). It brings quantitative bounds in our analysis but, nevertheless, gives the correct qualitative behavior and facilitates the physical insight into the problem. Using two different approaches from Refs. [5,6] MV configurations with three and five components in Eq. (1) were checked. This resulted in 1) a reduction of the region of existence of metastable MV states at the low magnetic field limit, 2) an appearance of additional unstable states corresponding to the saddle points of the free energy function, and 3) no new vortex configurations in the ground state. Thus, two components in Eq. (1) are sufficient to describe the vortex structure in the ground state of our system. Depending on the radial state of the components we defined two different configurations: *giant-giant* ($n_1 = n_2 = 0$) and *giant-ring* ($n_1 = 0, n_2 = 1$) MV states. The first represents a combination of two GV states while the second is composed of one giant and one ring vortex.

III. CENTERED STEP-LIKE MAGNETIC FIELD

First, we investigate the case of a centered step-like magnetic field corresponding to a magnetic disk. The effect of the size of the superconducting disk on the vortex state is shown in the phase diagram of Fig. 2. The parameters considered are $R_1 = 4.5\xi$ and $R_2 = 6.0\xi$. The solid lines indicate where the ground state of the free energy changes from one state to another and dashed lines correspond to transitions between different GV states as metastable states. The right axis of the diagram shows the corresponding positive flux through the region $\rho < R_1$.

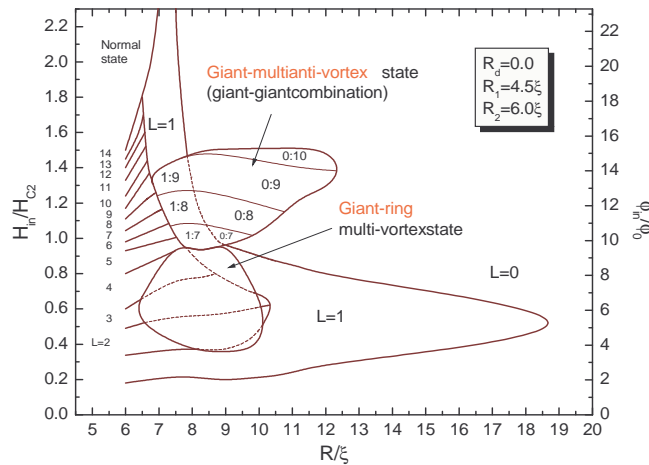


FIG. 2. The $H_{in} - R$ phase diagram for the ground state of a thin superconducting disk in a step-like magnetic field. Solid curves indicate transitions between different vortex states including different MV regions. Dashed curves denote the transitions between different metastable GV states.

One can clearly see the *re-entrant* behavior. For example, for $R = 9.0\xi$ we observe the following change of total vorticity $L = 0 \rightarrow 1 \rightarrow 2 \rightarrow 3 \rightarrow 1 \rightarrow 0$. Notice that the ground state with total vorticity $L = 0$ and $L = 1$ covers the largest part of the phase diagram. With increasing disk size, all other *GV* states are strongly suppressed in favor of the various *MV* states. For small disk sizes different *GV* states are present as the ground state. But with increase of disk size, islands with different *MV* configurations (*giant-ring* and *giant-giant* *MV* states) dominate the ground state diagram. For $R = 6.38\xi$, a giant-ring *MV* state appears, and for $R = 6.7\xi$ we obtain giant-giant states.

As one can see in Fig. 2, for example, for $R = 9.0\xi$ and with increasing magnetic field H_{in} , giant-giant combinations $(L_1 : L_2) = (0 : 7), (0 : 8), (0 : 9)$ etc. become the ground state. In the contour plot of the $|\psi|^2$ -distribution for these states we observe single vortices which are arranged on a ring with a low density area (see Fig. 3(a), blue color - zero density, red - highest density) situated in the center of the disk (see Fig. 3(a), for the $(0 : 7)$ state). This central area is associated with a giant vortex, and encircling it leads to a phase change showing the vorticity $L = 7$.

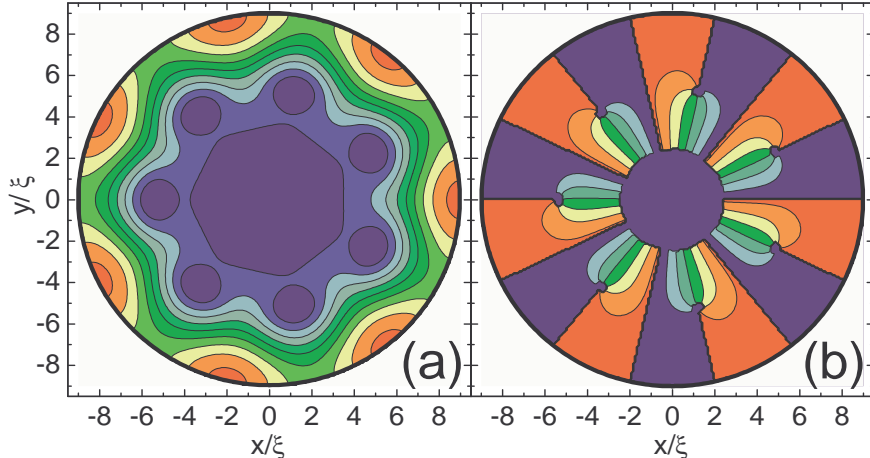


FIG. 3. (a) Contour plot of the superconducting density for the $(0 : 7)$ *giant-multi anti-vortex* ground state, and (b) the corresponding contour plot of the phase. Notice that the phase near the boundary is near 0 (blue) or 2π (red) but due to the finite numerical accuracy it oscillates between $2\pi - \varepsilon$ and $2\pi + \varepsilon$ where $\varepsilon \approx 10^{-5}$.

Fig. 3(b) shows the contour plot of the corresponding phase with seven anti-vortices arranged in a circle around the giant vortex and the *total* vorticity is $L = 0$. It is important to emphasize that for the disk size $R = R_2$ and with changing of R_1 *giant-giant* *MV* states consist only of vortices arranged radially symmetric with no anti-vortices present. Thus, it is obvious that enlarging the superconducting disk enhances the influence of the negative part of the step-like magnetic field. As a result we obtain a new giant-giant form called *giant-multi anti-vortex* states. The total vorticity is now equal to the lowest vorticity of the giant vortex states of which the multi-vortex consists of. This inevitably leads to a re-entrant behavior in the total vorticity, which is in agreement with Ref. [10] where it was found numerically that several vortices can enter (or exit) at once for disks with sufficiently large radius. For $R = R_2$ disks we only found that $L \rightarrow L \pm 1$ transitions are possible. With increase of the disk radius the $(0 : 8)$ and $(0 : 9)$ *giant-multi anti-vortex* states become $(1 : 8)$ and $(1 : 9)$, respectively. For $R > 12.33\xi$, the multi-vortex states become metastable again and the $L = 0$ and $L = 1$ states are now the only ground states. Moreover, for $R > 18.67\xi$ we have the Meissner state for all values of the applied magnetic field.

IV. SHIFTED STEP-LIKE MAGNETIC FIELD

Next, we move the step-like field profile along the radius of the superconducting disk, i.e. consider a ring magnetic field profile as in the case of a current loop. In Fig. 4, we present the phase diagram as function of R_d . The parameters of the magnetic field profile are $R_1 - R_d = 4.5\xi$, $R_2 - R_d = 6.0\xi$, and $R = 9.0\xi$. Thick solid curves indicate the transitions between different vortex states and dashed lines denote transitions between metastable *GV* states.

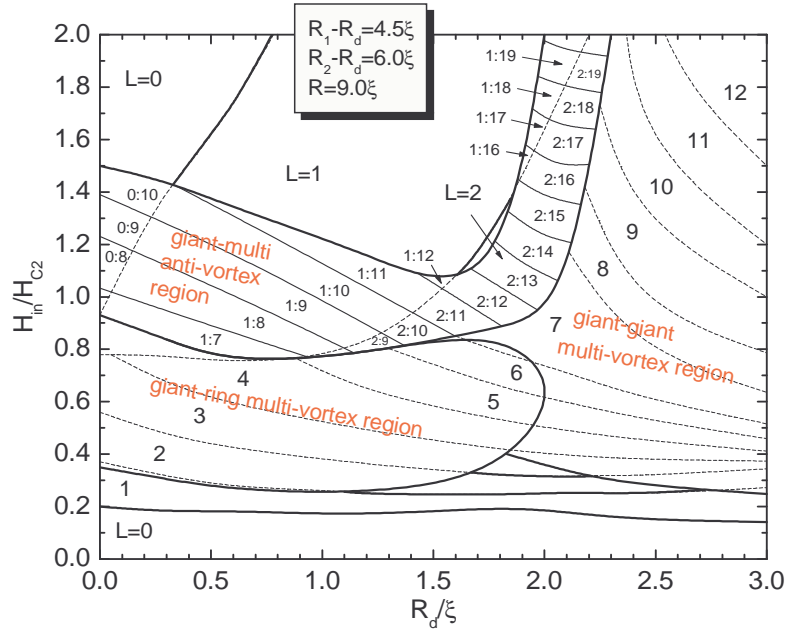


FIG. 4. The $H_{in} - R_d$ phase diagram for the ground state of a thin superconducting disk in a ring step-like magnetic field distribution. The same curve convention is used as in Fig. 2.

The *re-entrant* behavior, as in previous case, is clearly visible. The most important result is that the *MV* states dominate this diagram. Moreover, we have both types of multi-vortices, i.e. *giant-giant* and *giant-ring*, as ground state, and with shifting the field profile towards the disk periphery, *giant-giant MV* configurations cover most of the superconducting region. The *giant-giant MV* states in this case appear both as states with no anti-vortices present, and as *giant-multi anti-vortex* states. Following the transition lines, a correspondence between different *giant-multi anti-vortex* states ($L_1 : L_2$) can be seen: L_2 remains the same, while L_1 increases from 0 to 2. As one can see, the latter is strongly correlated with *re-entrant* behavior. In the rest of the diagram, the *MV* states with the "classical" geometry (both *giant-giant* and *giant-ring*) dominate. However, a difference between those states exists. As shown in Fig. 5, in the case of a *giant-ring* state, vortices are preferentially distributed within a ring-shaped lower density area. Further, considering the high density areas at the disk periphery, a shift in phase of $\Delta\theta = \pi/L$ is observed, where L is the total vorticity. Although these states have a different origin sometimes they can exhibit a similar distribution of vortices but the phase is always able to distinguish between them.

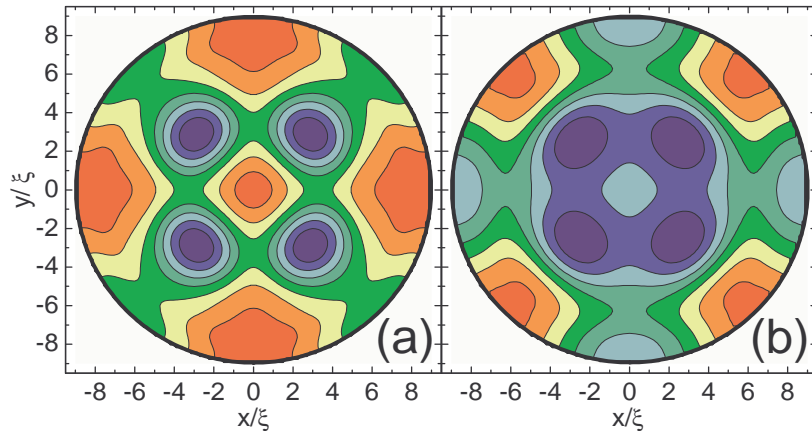


FIG. 5. Contour plots of the superconducting wave density for *giant-giant* (a) and *giant-ring* (b) *MV* state with the total vorticity $L = 4$.

ACKNOWLEDGEMENTS

This work was supported by the Flemish Science Foundation (FWO-VI), the Belgian Inter-University Attraction Poles (IUAP-IV), the “Onderzoeksraad van de Universiteit Antwerpen” (GOA), and the ESF programme on “Vortex matter”.

* Corresponding author. *E-mail address:* milo@uia.ua.ac.be

Permanent address: Donetsk Physical & Technical Institute, National Academy of Sciences of Ukraine, Donetsk 83114, Ukraine

- [1] A. K. Geim, I. V. Grigorieva, S. V. Dubonos, J. G. S. Lok, J. C. Maan, A. E. Filippov, and F. M. Peeters, *Nature (London)* **390**, 259 (1997).
- [2] V. A. Schweigert and F. M. Peeters, *Phys. Rev. B* **57**, 13817 (1998).
- [3] V. A. Schweigert, F. M. Peeters, and P. S. Deo, *Phys. Rev. Lett.* **81**, 2783 (1998).
- [4] J. J. Palacios, *Phys. Rev. B* **58**, R5948 (1998).
- [5] V. A. Schweigert and F. M. Peeters, *Phys. Rev. Lett.* **83**, 2409 (1999).
- [6] S. V. Yampolskii and F. M. Peeters, *Phys. Rev. B* **62**, 9663 (2000).
- [7] H. J. Fink and A. G. Presson, *Phys. Rev.* **151**, 219 (1966).
- [8] J. Govaerts, G. Stenuit, D. Bertrand, and O. van der Aa, *Phys. Lett. A* **267**, 56 (2000).
- [9] M. J. Van Bael, L. Van Look, K. Temst, M. Lange, J. Bekaert, G. Guentherodt, V. V. Moshchalkov, and Y. Bruynseraede, *Physica C* **332**, 12 (2000).
- [10] V. A. Schweigert and F. M. Peeters, *Physica C* **332**, 266 (2000).